A Novel Electrochemical Sensor Based on Reduced Graphene Oxide–TiO$_2$ Nanocomposites with High Selectivity for the Determination of Hydroxychloroquine

Huilan Zhang[a], Lu Cheng[a], Hongyuan Shang[b], Wen Zhang[a], and Aiping Zhang[a], *

[a] College of Pharmacy, Shanxi Medical University, Taiyuan, Shanxi, 030001 P. R. China
[b] College of Chemistry, Chemical Engineering and Materials Science, Soochow University, Suzhou, 215123 PR China
*e-mail: zhangap1@163.com

Abstract—A simply sensitive sensor based on a reduced graphene oxide–TiO$_2$ nanocomposite modified glassy carbon electrode (RGO–TiO$_2$/GCE) was developed for the electrochemical determination of an antimalarial drug, hydroxychloroquine (HCQ). The modified electrode was characterized by cyclic voltammetry (CV) and electrochemical impedance spectroscopy (EIS). Electrochemical test showed that the RGO–TiO$_2$ electrode had stronger electrochemical activity and higher effective real surface area than that of TiO$_2$ electrode and bare electrode. The electrochemical response of RGO–TiO$_2$ nanocomposite modified electrode toward HCQ oxidation was studied by CV, chronoamperometry (CHA), chronocoulometry (CHC) and square-wave voltammetry (SWV). Interestingly, RGO–TiO$_2$/GCE indicated an excellent electrocatalytic activity for HCQ. Under the optimal experimental conditions, a linear relationship between the peak current and the concentration was obtained, ranging from 0.25 to 500 µM, with the detection limit (S/N = 3) of 12.5 nM and quantification limit (S/N = 10) of 0.97 µM. Furthermore, the proposed sensor was successfully applied to the determination of HCQ in pharmaceutical (tablets) samples. In summary, the developed sensor was low cost and efficient, making it potentially attractive for practical sample analysis application of HCQ.

Keywords: hydroxychloroquine, RGO–TiO$_2$ nanocomposites, electrochemical sensor, determination, square-wave voltammetry

DOI: 10.1134/S1023193521080152

INTRODUCTION

Hydroxychloroquine (HCQ) is an effective antimalarial drug that has been widely used as an inhibitor of malaria prevention and treatment for decades. It is also used to treat rheumatoid arthritis and similar collagen diseases, as well as amoebic hepatitis [1]. In particular, HCQ can be used as a treatment for the novel Corona Virus Disease 2019 (Covid-19) under conditions where there is currently no therapeutic vaccine or specific antiviral drugs [2]. However, HCQ has a prolonged half-life and large individual differences. Long-term use of HCQ can also induce some serious adverse reactions or accumulation of poisoning [3, 4]. Therefore, clinical monitoring of plasma concentration of HCQ is important for optimizing treatment and controlling side effects. Because higher doses cause side effects and toxicity, lower doses reduce or even lose the desired effect. It is imminent to develop a simple, fast and accurate analytical method for identifying and quantifying hydroxychloroquine in pharmaceutical and biological samples.

Various techniques have been utilized for HCQ detection, including non-aqueous titration, spectro-photometry, electrochemical sensors and high performance liquid chromatography [5–12]. However, compared to electrochemical sensors, other techniques usually require complicated pre-processing steps, expensive equipments or skilled operators. In order to overcome these inherent disadvantages, electrochemical methods may be a good alternation since they are usually performed using simple instruments and also can reduce the cost and time required for analysis. Importantly, electrochemical methods for the determination of HCQ drugs have so far been rarely reported [12–15].

Nanomaterials with unique physical and chemical properties and exceptional biomolecular binding capabilities make a significant contribution to increasing sensing surface area and improving detection sensitivity. TiO$_2$ nanoparticles (NPs) have been widely used in many aspects, including photocatalysis, sensors and biomedical science, etc, due to their broad photocatalytic effect, stability, porosity, wide bandgap, crystalline, high surface area, high adsorption and low toxicity [16, 17]. Unfortunately, catalytic activity of TiO$_2$ NPs is limited by the aggregation of NPs and

fast recombination of electron-hole pair. In order to protect TiO$_2$ NPs from aggregation in a physiological environment and ensure their uniform distribution and enhance the catalytic activity, we employed reduced graphene oxide (RGO) as a modifier for HCQ analysis in electrochemical sensors [18−21]. RGO-based hybrid composites have several advantages, such as large surface area, excellent electrical conductivity as well as easy preparation. In addition, RGO provides a large surface area for attachment to other materials, making it a suitable candidate as the support material, binding more TiO$_2$ NPs which are highly dispersed onto RGO sheets, thereby improving their electrochemical properties as well as realizing a uniform distribution without aggregation.

In this work, we intend to modify the glassy carbon electrode (GCE) with RGO−TiO$_2$ NPs and electrochemically characterize it, as shown in Scheme 1. The electrochemical behavior of HCQ on the modified electrode was studied by electrochemical impedance spectroscopy, cyclic voltammetry, square-wave voltammetry and chronoamperometry. Electrochemical sensor was applied to the determination of HCQ in commercial and urine samples by standard addition methods. A accurate and specific RGO−TiO$_2$ electrochemical sensor for the detection of HCQ was explored. This work will open up new opportunities for developing novel, convenient, accurate and specific electrochemical sensors for the detection of drugs.
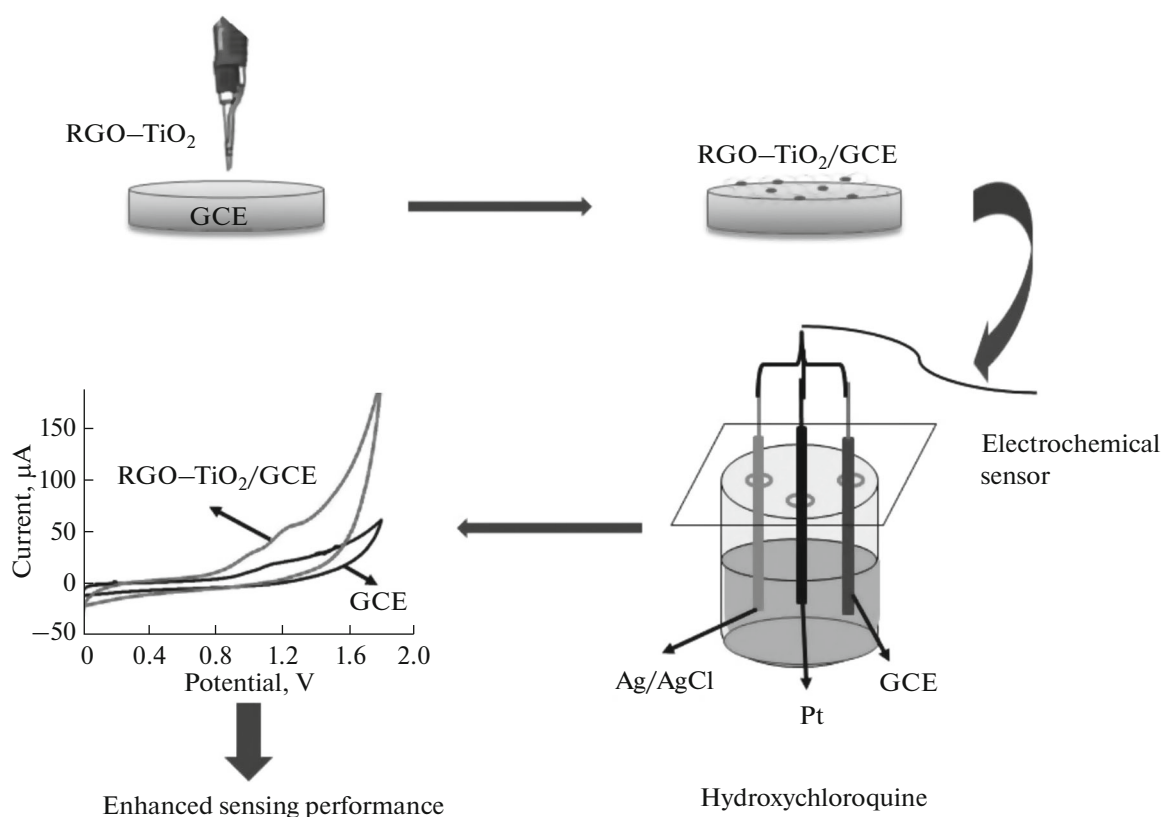
**Scheme 1.** Schematic representation of the proposed RGO−TiO$_2$/GCE sensor.

EXPERIMENTAL

Reagents and Apparatus

RGO−TiO$_2$ NPs were prepared and characterized early by research group [22]. HCQ was purchased from National Institutes for Food and Drug Control. All other chemicals and reagents were of analytical grade or better and used without further purification. Phosphate buffer saline (PBS) with various pH was prepared by mixing 0.1mol L^{-1} KH$_2$PO$_4$ and 0.1 mmol L^{-1} Na$_2$HPO$_4$ in different ratios. Double distilled (DI) water was used throughout the experiments. The stock solution of HCQ (1 × 10^{-3} M) was prepared with 0.2 M PBS (pH 8.00) and stocked at 4°C in the dark. Working standard solutions were prepared by appropriate dilution of the stock standard solution with buffer.

Electrochemical measurements were carried out on a CHI660D electrochemical workstation (CHI Instrument Company, Shanghai, China). All electro-
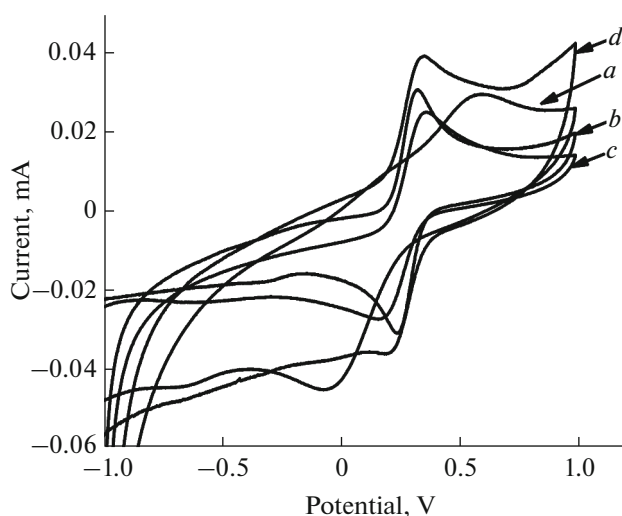
Fig. 1. CV curves of GCE (*a*), TiO$_2$/GCE (*b*), 40% RGO–TiO$_2$/GCE (*c*) and 50% RGO–TiO$_2$/GCE (*d*) in the solution of 5 mM Fe(CN)$_6^{3-/4-}$ at 50 mV s^{-1}.

chemical experiments were carried out with a three electrode system comprising glassy carbon electrode (GCE, 3 mm diameter) as the working electrode, a platinum (Pt) wire as an auxiliary electrode and an Ag/AgCl (3 M KCl) as a reference electrode. pH measurements were performed using a 691 pH meter (Metrohm, Switzerland) to adjust the pH of the buffer solution, which was used as a supporting electrolyte in voltammetric experiments.

Preparation of Modified Glassy Carbon Electrode

Before modification, the bare GCE was polished with 0.05 μm alumina slurries until a mirror-like surface was obtained. It was rinsed ultrasonically with 1 : 1 HNO$_3$, ethanol, and deionized water, respectively, and dried at room temperature. RGO–TiO$_2$ was ultrasonically dispersed in N,N-dimethylformamide (DMF) (1 mg mL^{-1}) for 30 min to form homogenous suspensions. The RGO–TiO$_2$/GCE electrode was prepared by casting 10 μL of RGO–TiO$_2$ suspension on the GCE surface and dried under an infrared lamp. Prior to use, the modified electrode was carefully rinsed with water to remove the loosely attached RGO–TiO$_2$ on the electrode, and dried in an air stream [23].

Electrochemical Measurements

Electrochemical characterization of RGO–TiO$_2$/GCE was carried out by cyclic voltammetry (CV) and electrochemical impedance spectra (EIS) in 0.1 M KCl containing 5 mM Fe(CN)$_6^{3-/4-}$. Electrochemical analysis of HCQ on RGO–TiO$_2$/GCE was carried out in a 0.1 M PBS (pH 8.00) solution. 10 mL of an electrolyte solution containing an appropriate amount of HCQ was added to an electrolytic cell in which the electrodes were immersed. The CV was scanned within a potential range of 0.0 to 1.2 V. The EIS was recorded within a frequency range from 0.1 to 10000 Hz with a pulse amplitude of 5 mV. All voltammetric measurements were carried out at ambient temperature (25°C). After each measurement, the modified electrode was washed with water and scanned in blank PBS until the electrochemical signal of HCQ completely disappeared.

Procedure for Pharmaceutical Analysis

The stock solutions of the tablet samples were prepared as follows: ten tablets of HCQ were accurately weighed and powdered in mortar. A portion of powdered tablet equivalent to the average weight of one tablet was transferred to a 100.0 mL beaker and dissolved in DI water, shaken well for 10 min, then the solution was filtered and made up to the mark with DI water to get the final concentration. Appropriate aliquots from the working solutions were taken for the voltammetric determination by CV techniques in the standard addition mode, and diluted with buffer to obtain the final concentrations within the calibration curve. Then solutions were determined as described under optimized procedure.

To prove that the proposed method was enough satisfactory and selective, the analysis of the same urine samples was carried out simultaneously with proposed methods. Urine samples were obtained from healthy volunteers abstained from any medications during the week preceding the study. Prior to voltammetric analysis, urine samples were filtered and diluted ten times with PBS solution. In this case, the standard addition method was employed in analysis of human urine samples [24].

RESULTS AND DISCUSSION

Characterization of Modified Electrode

Figure 1 showed typical cyclic voltammograms of different electrodes in 5 mmol L^{-1} Fe(CN)$_6^{3-/4-}$. A pair of redox peaks was observed in each CVs, which was ascribed to the redox of Fe(CN)$_6^{3-/4-}$. Compared with bare GCE, TiO$_2$/GCE and 40% RGO–TiO$_2$/GCE, the current in 50% RGO–TiO$_2$/GCE increased significantly, indicating that the introduction of RGO–TiO$_2$ could accelerate the electron transfer and enhance electric conductivity.

Electrochemical impedance spectroscopy (EIS) was further used to evaluate the electron transfer performance of different modified electrodes in 5 mmol L^{-1} Fe(CN)$_6^{3-/4-}$. Nyquist plots obtained were shown in Fig. 2. This equivalent circuit includes solution resis-
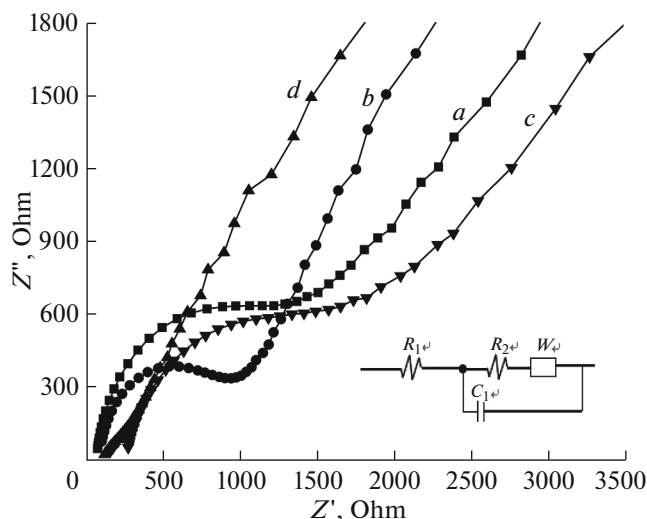
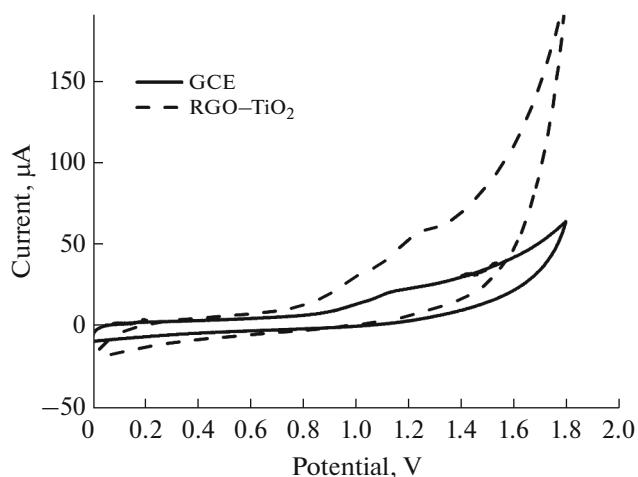**Fig. 2.** Nyquist plots of EIS of bare GCE (*a*), TiO$_2$/GCE (*b*), 40% RGO–TiO$_2$/GCE (*c*) and 50% RGO–TiO$_2$/GCE (*d*) in 5 mM Fe(CN)$_6^{3-/4-}$ solution, and the frequency range is at 0.01 Hz–10 kHz (the insert is the equivalent circuit of the Nyquist plots).

Fig. 3. CV curves of 0.2 mM HCQ on bare GCE and RGO–TiO$_2$/GCE in 0.1 M PBS of pH 6.00. Scan rate: 600 mV s^{-1}.

tance (R_1), electron transfer resistance (R_2), constant-phase element (CPE$_1$), and Warburg impedance (W_1), as shown in the inset of Fig. 2. The Nyquist plot of impedance spectra consists of a semicircle portion that is associated with the electron transfer limited process at higher frequencies, and a linear portion associated with the diffusion process at lower frequencies. The electron transfer resistance (R_2) can be evaluated by using the diameter of the semicircle. As shown in Fig. 2, 50% RGO–TiO$_2$/GCE displayed almost a straight line in the Nyquist plot, thereby exhibiting a lower Ret than bare GCE, TiO$_2$/GCE and 40% RGO–TiO$_2$/GCE. These results were well consistent with the phenomena in CVs, hence confirming that 50% RGO–TiO$_2$/GCE had better electrochemical properties and higher electrocatalytic activity.

Electrochemical Behavior of HCQ on Bare GCE and Modified GCE

Figure 3 shows the cyclic voltammograms of 0.2 mM HCQ on bare GCE and RGO–TiO$_2$/GCE surface in 0.1 M PBS of pH 6.00. It can be seen that HCQ showed one and two oxidation peaks on bare GCE and RGO–TiO$_2$/GCE, respectively. The first anodic peak did not show sufficient sensitivity, so the second anodic peak was used in the further studies. The anodic peak currents (I_{pa}) of HCQ on bare GCE and RGO–TiO$_2$/GCE were measured to be 19.5 and 40.2 μA, respectively. Two times increased in current sensitivity was observed for HCQ oxidation on RGO–TiO$_2$/GCE. The results suggested that RGO–

TiO$_2$/GCE possessed higher electrochemical activity for HCQ.

OPTIMIZATION OF EXPERIMENTAL CONDITIONS

Effect of pH

The pH value of the supporting electrolyte is an important factor in determining the performance of electrochemical sensors. Therefore, the effect of pH on the electrochemical behavior of HCQ on RGO–TiO$_2$/GCE was investigated by CV and SWV for 50.0 μM HCQ in 0.1 M PBS of different pH ranging from 6.00 to 7.95 (Figs. 4a and 5a). As shown in Figs. 4a and 5a, it was clear that changing pH altered both the peak current and the peak potential of HCQ. Thus, the anodic peak potential (E_{pa}) of HCQ on the RGO–TiO$_2$/GCE depends on the pH of the buffer solution and protonation/deprotonation participates in the charge transfer process. The relationship between the anodic peak potential and the solution pH value was demonstrated in Figs. 4b and 5b. This relationship could be fit to the linear regression and was subject to the following equations:

CV curves: $E_{pa}(V) = -0.0672pH + 1.353$
$(R^2 = 0.9950)$ peak 1;

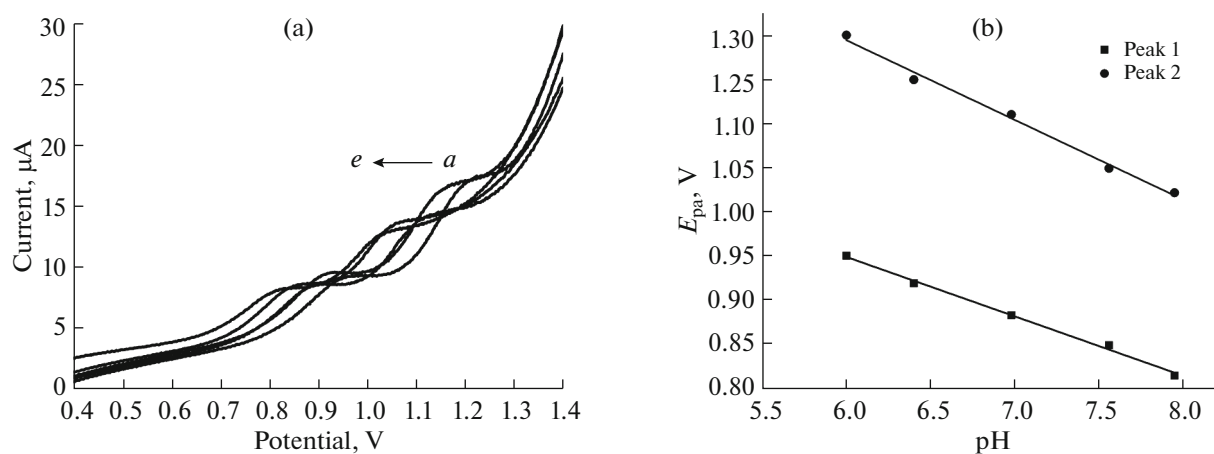$E_{pa}(V) = -0.0901pH + 1.736$
$(R^2 = 0.9904)$ peak 2;

SWV curves: $E_{pa}(V) = -0.0746pH + 1.448$
$(R^2 = 0.9951)$ peak 1;

Fig. 4. (a) Cyclic voltammograms of HCQ (50 µM) at different pH: ($a \rightarrow e$: 6.00, 6.40, 6.98, 7.56, 7.95). (b) The relationship between the anodic peak potentials and pH values. Scan rate: 50 mV s^{-1}.
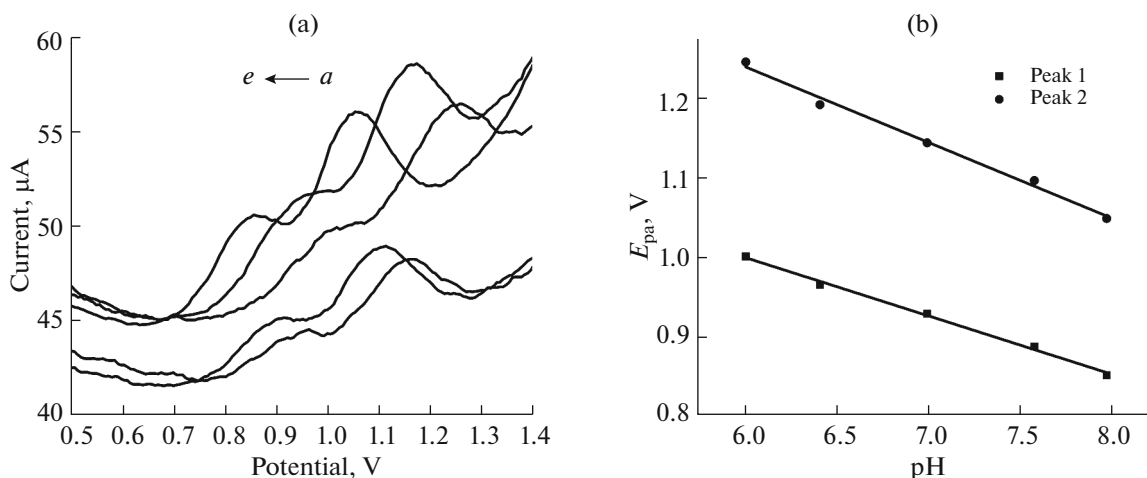
Fig. 5. (a) SWV graphs of HCQ (50 µM) at different pH: ($a \rightarrow e$: 6.00, 6.40, 6.98, 7.56, 7.95). (b) The relationship between the anodic peak potentials and pH values. Scan rate: 600 mV s^{-1}.

$$E_{pa}(V) = -0.0967pH + 1.822$$
$$(R^2 = 0.992) \text{ peak 2.}$$

The slope of the peak 1 was calculated to be 67.2 and 74.6 mV pH^{-1}, which are close to the theoretical value of 59 mV pH^{-1} from the Nernst equation for an equal number of proton and electron transfer process. And higher current response of HCQ was obtained at pH 6.00. Therefore, a PBS buffer of pH 6.00 was chosen as the supporting electrolyte solution in further research work.

Effect of Scan Rate

The effect of scan rate on the oxidation peak current of HCQ was examined on RGO–TiO$_2$/GCE (Fig. 6a). Figure 6a showed the CV curves of the RGO–TiO$_2$ modified electrode measured at various scan rates of 30 to 600 mV s^{-1} in 0.1 M PBS (pH 6.00) containing 100 µM HCQ.

According to the Fig. 6b, the peak current (I) increased linearly with the increase of square root of scan rate ($v^{1/2}$) ranging from 30 to 600 mV s^{-1}, which could be expressed as: $I_p(\mu A) = 6.048 \, v^{1/2}(mV/s^{1/2}) - 17.245$; $R^2 = 0.9899$. Therefore, it can be concluded that the oxidation peak current of HCQ is a diffusion-controlled process on the surface of RGO–TiO$_2$/GCE.

The plots of oxidation peak current (log I) vs. log scan rate (log v) showed a good linear relationship with a slope of 0.630 (Fig. 6c), which was almost equal to the theoretical value of 0.5 for a purely diffusion-controlled process. The results showed that the oxidation of
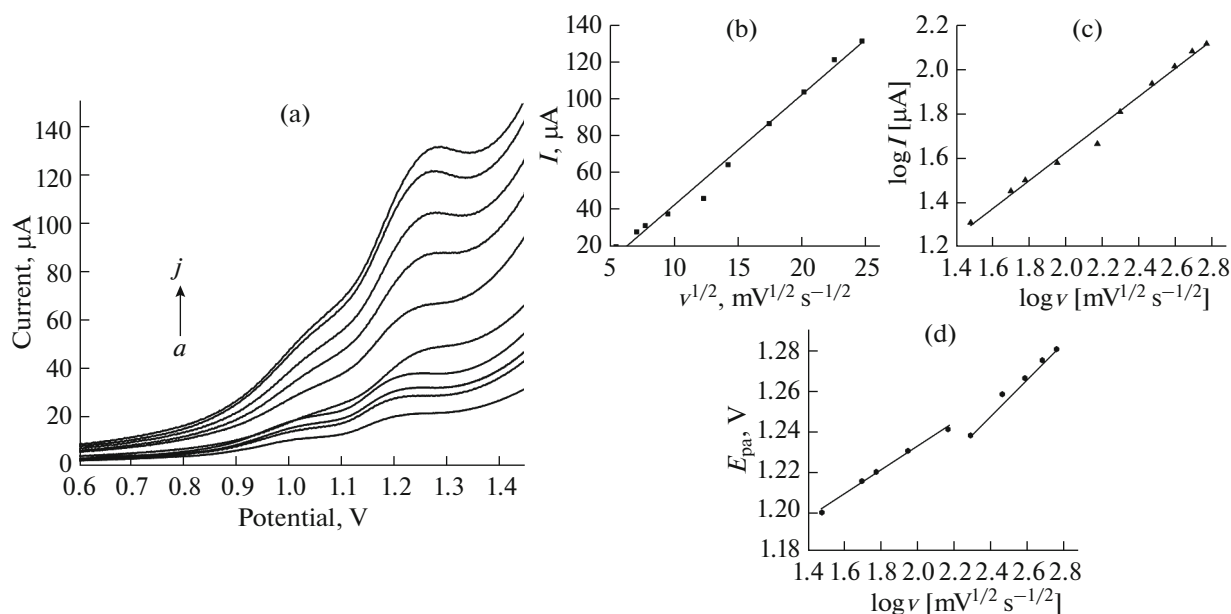
Fig. 6. (a) Cyclic voltammograms of HCQ ($100 \, \mu M$) in 0.1 M PBS solution (pH 6.00) on RGO–TiO$_2$/GCE at different scan rates from 30 to 600 mV s^{-1}. (b) The plot of I versus $v^{1/2}$. (c) The plot of $\log I$ versus $\log v$. (d) The plot of E_{pa} versus $\log v$.

HCQ on RGO–TiO$_2$/GCE was mainly controlled by diffusion, which was supported by adsorption.

The E_p of the oxidation peak also depends on the scan rate. As the scan rate increased, the peak potential shifted to a more positive value, indicating that the oxidation process is irreversible. A linear relationship between the peak potential and the log scan rate (Fig. 6d) was observed when the scan rate was less than 150 mV s^{-1}. As for the irreversible reaction of HCQ, E_p is defined by the Laviron's equation [25]:

$$E_{pa} = E^{\ominus} + \frac{2.303RT}{\alpha nF} \log \frac{RTk_s}{\alpha nF} + \frac{2.303RT}{\alpha nF} \log v.$$

Where α is the transfer coefficient, k_s is the standard heterogeneous rate constant, n is the number of transfer electron, v is the scan rate, and $E^{\ominus}$ is the formal transfer potential. Thus, the value of $2.303RT/\alpha nF$ can be easily calculated from the slope of above-mentioned line. In this system, the slope is 0.059 and other parameters have their usual meaning, so αn is calculated to be 1.00. Since for a totally irreversible electron transfer, α is supposed to be 0.5, then n was calculated to be 2, indicating that two electrons were involved in the oxidation of HCQ.

By considering the slight shift in the peak potential relative to the bare electrode and TiO$_2$/GCE, the observed enhancement in voltammetric response on RGO–TiO$_2$/GCE was attributed to the increase in surface area of the electrode and the adsorption of the analyte on the surface of the modified electrode. Therefore, the electro-active surface area of bare GCE

and RGO–TiO$_2$/GCE was obtained by CV technique (Fig. 7), based on the Randles−Sevcik equation using 1.0 mM Fe(CN)$_6^{3-/4-}$ [26]:

$$I_p = \pm 0.446 \, nFA_{real}c\sqrt{\frac{nFDv}{RT}}.$$

Where I_p refers to the peak current of the anode, n is the number of electron transfer, F is the Faraday constant (C mol^{-1}), R is the universal gas constant, T is the temperature in Kelvin, A is the microscopic surface area of the electrode (cm^2), D is the diffusion coefficient (cm^2 s^{-1}), c is the bulk concentration of Fe(CN)$_6^{3-/4-}$ (mol cm^{-3}) and v is the scan rate (V s^{-1}).

For 1 mM Fe(CN)$_6^{3-/4-}$, $n = 1$ and $D = 7.60 \times 10^{-6}$ cm^2 s^{-1}, the effective surface areas of GCE, TiO$_2$/GCE and RGO–TiO$_2$/GCE were calculated and found to be 0.0207, 0.0457, 0.0861 cm^2, respectively. From the above results, it can be seen that the surface area of the electrode was significantly increased after the modification. The surface area was used to calculate the diffusion coefficient of 500 μM HCQ and found to be 2.37×10^{-5} cm^2 s^{-1}.

Diffusion Coefficient of HCQ on the Electrode Surface

Chronoamperometry (CHA) is a common method for studying the diffusion characteristics of chemically modified electrodes. Chronoamperometric analyses of HCQ on RGO–TiO$_2$/GCE were carried out by setting the working electrode potential at 1.00 V vs.
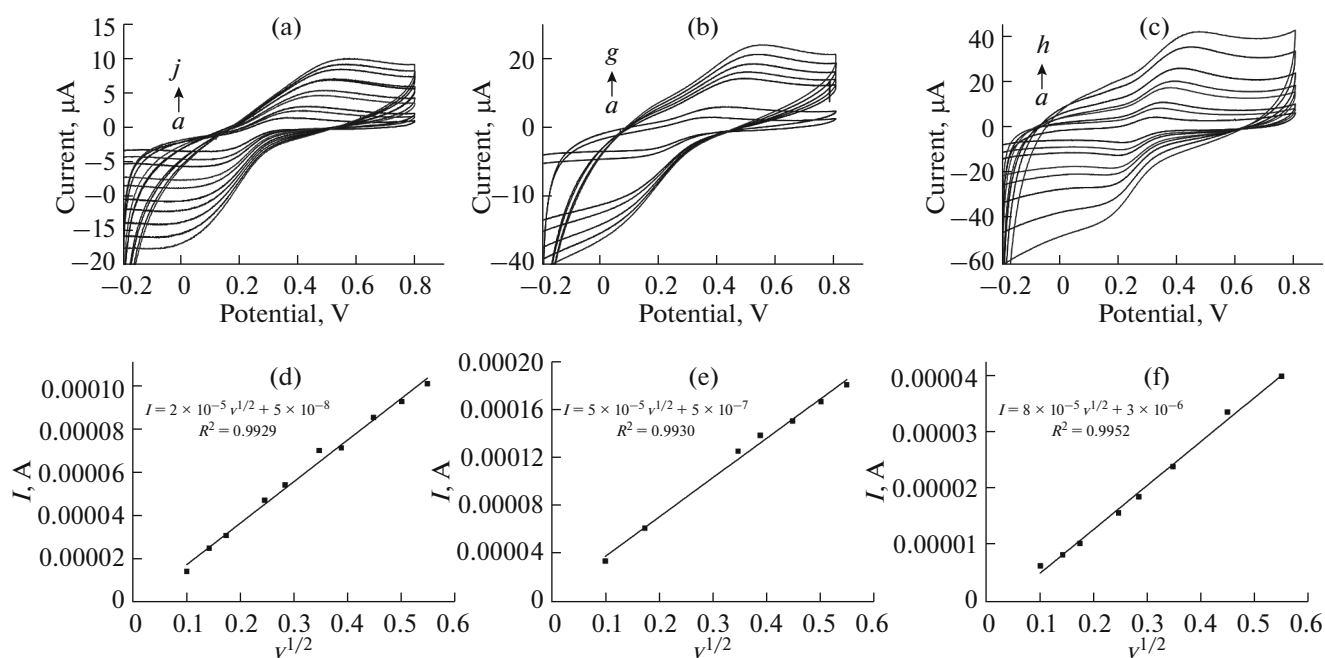
Fig. 7. Cyclic voltammograms of $Fe(CN)_6^{3-/4-}$ (1.0 mM) in 0.1 M PBS solution (pH 6.00) on bare GCE (a), TiO_2/GCE (b) and RGO–TiO_2/GCE (c) at different scan rates from 10 to 300 mV s^{-1}. The plot of I versus $v^{1/2}$ on bare GCE (d), TiO_2/GCE (e) and RGO–TiO_2/GCE (f).

Ag/AgCl for the various concentrations of HCQ in 0.1 M PBS solution (Fig. 8). The diffusion coefficient (D) of HCQ on the surface of a 50 wt % RGO–TiO_2/GCE electrode can be calculated by the Cottrell equation:

$$I = nFAD^{1/2}c\pi^{-1/2}t^{-1/2},$$

where I is the current (A), n is the number of electrons involved in the process, F is the Faraday constant, A is the area of the electrode (cm^2), c is the bulk concentration (mol cm^{-3}), D is the diffusion coefficient (cm^2 s^{-1}) and t is time (s).

The diffusion coefficient can be easily calculated from the slope of the plot of I vs. $t^{-1/2}$. Figure 8b showed the fitted experimental plots for different concentrations of HCQ. The slopes of the resulting straight lines were then plotted against HCQ concentration (Fig. 8c) and the mean value of D was determined to be 5.32×10^{-4} cm^2 s^{-1}.

The diffusion coefficient can also be calculated using CHC. In CHC, the charge response under diffusion control was described by the Cottrell equation:

$$Q = 2nFAD^{1/2}c\pi^{-1/2}t^{1/2}.$$

Figure 9b showed the experimental plots of Q vs. $t^{-1/2}$ with the best fit for different concentrations of HCQ employed. Figure 9c showed the relationship between

slopes of the resulting straight lines and the HCQ concentration, which was described by:

$$\text{Slope} = 0.2107c_{HCQ} + 8.290 \ (R^2 = 0.9941).$$

From these plots and by using the Cottrell equation, we calculated average diffusion coefficients of 5.1×10^{-4} cm^2 s^{-1}. This value is consistent with the diffusion coefficient obtained from the CHA measurement.

Calibration Curve

Under the optimal conditions, the calibration curve of HCQ on the RGO–TiO_2 modified electrode was recorded by SWV technique. Fig. 10a showed the SWV curves for the consecutive additions of concentrations of HCQ over the range of 2.5×10^{-7} to 5.0×10^{-4} M in PBS of pH 6.00. It can be seen that as the concentration of HCQ increased, the oxidation peak signals increased linearly. The calibration curve of HCQ revealed two linear responses (Fig. 10b):

$$I_{pa} = 0.311c_{HCQ} + 39.161 \ (R^2 = 0.9946)$$

and

$$I_{pa} = 0.084c_{HCQ} + 54.701 \ (R^2 = 0.9943).$$

According to IUPAC, the limit of detection (LOD) and the limit of quantification (LOQ) were calculated using the following equations: $LOD = 3S/m$ and
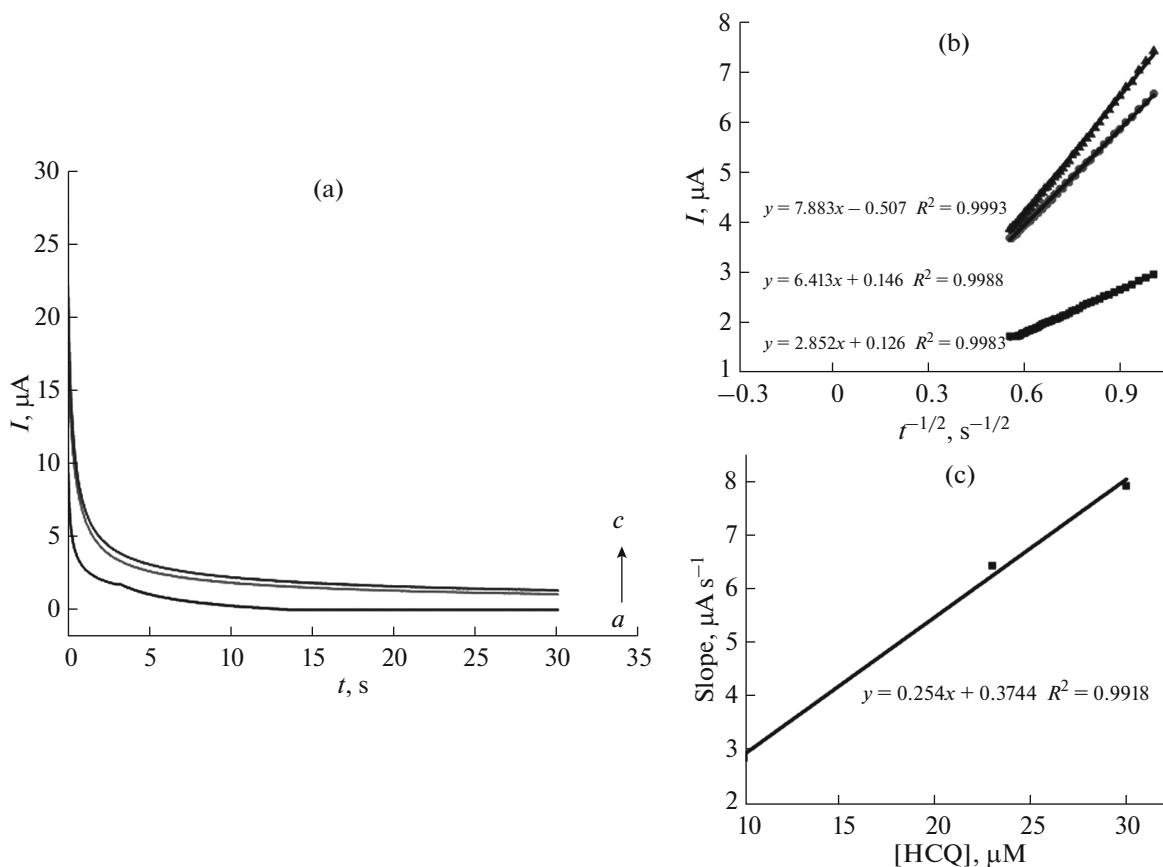
Fig. 8. (a) CHA curves of different concentrations of HCQ in 0.1 M PBS solution (pH 6.00) on RGO–TiO$_2$/GCE. Working potential is 1.0 V; $a \to c$: 10, 23, 30 µmol L^{-1}. (b) Plot of oxidation peak current (I) vs. $t^{-1/2}$. (c) Plot of the slope of the straight lines vs. the concentration of HCQ.

LOQ = $10S/m$. Where S is the blank standard deviation and m is the slope of the calibration curve, so LOD and LOQ were found to be 1.25×10^{-8} and 9.47×10^{-7} M, respectively.

Based on the application of different chemically modified electrodes reported in the literature (Table 1), we demonstrated that the proposed sensor performed well in detecting HCQ with wider linear ranges and higher limits of detection. Therefore, RGO–TiO$_2$/GCE is a competitive candidate in the determination of HCQ compared with other modified electrodes.

*Selective Determination of HCQ
in the Presence of Ascorbic Acid (AA)*

To the best our knowledge, there is no report on the determination of HCQ in the presence of AA using RGO–TiO$_2$ modified electrode. Therefore, the main aim of this study was to detect HCQ and AA simultaneously on the surface of the modified electrode using SWV technique. This was performed by alternatively changing the concentrations of HCQ in the presence of 100 µM of AA and recording their SWV signals (Fig. 11). Based on these voltammograms, three well-distinguished anodic peaks +0.2, +0.9, and +1.20 V were observed, corresponding to the oxidation of AA

Table 1. Comparison with other published chemically modified electrodes

Electrode	Method	LOD, nmol L^{-1}	Liner range, mol L^{-1}	Ref.
CPT-BDD electrodes	SWV	60	1×10^{-7}–1.9×10^{-6}	[27]
MWCNTs/CPE	DPV	6.0	5.7×10^{-8}–1×10^{-4}	[13]
GC/PAPA SAM	DPV	4.5	5.0×10^{-8}–12.3×10^{-6}	[14]
RGO–TiO$_2$/GCE	SWV	12.5	2.5×10^{-7}–5.0×10^{-4}	
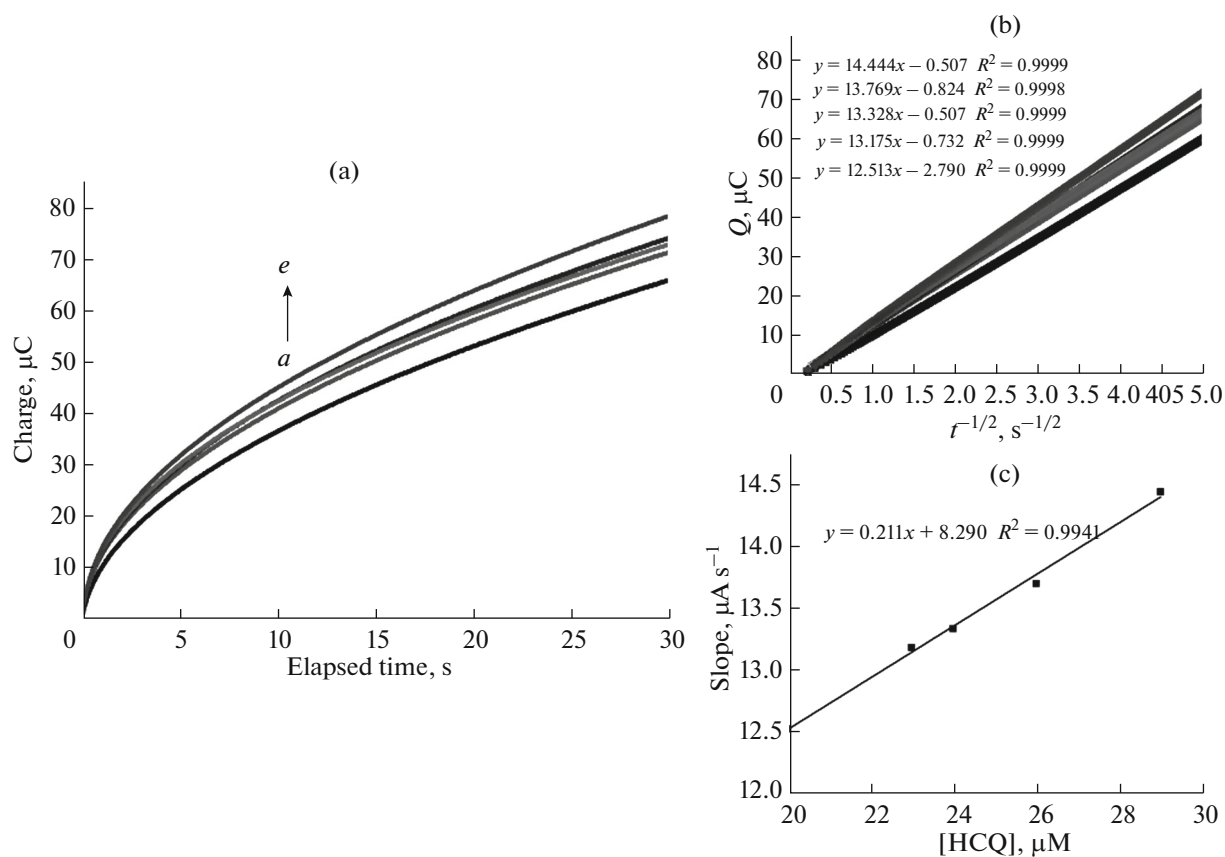
Fig. 9. (a) CHC curves of different concentrations of HCQ in 0.1 M PBS solution (pH 6.00) on RGO–TiO$_2$/GCE. Working potential is 1.0 V; $a \rightarrow e$: 10, 23, 24, 26, 29 µmol L^{-1}. (b) Plot of oxidation charge (Q) and $t^{-1/2}$. (c) Plot of the slope of the straight lines vs. the concentration of HCQ.
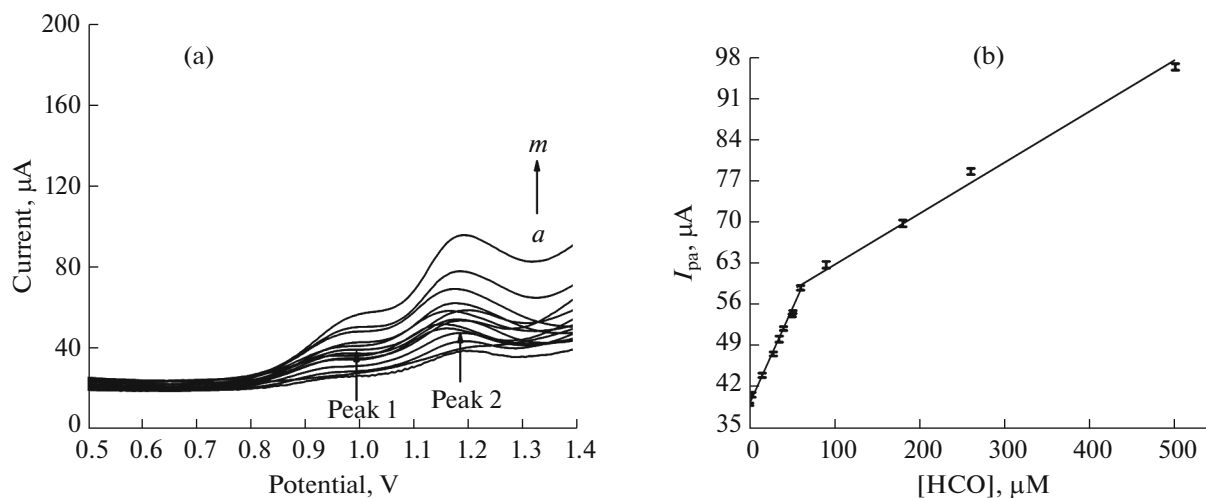
Fig. 10. (a) SWV curves recorded on RGO–TiO$_2$/GCE in 0.1 M PBS solution (pH 6.00) after addition of HCQ to give final solution concentrations in the range of 2.5×10^{-7}–5.0×10^{-4} M. Scan rate: 600 mV s^{-1}. (b) The calibration plots of the peak current vs. the concentration of HCQ ($n = 3$).
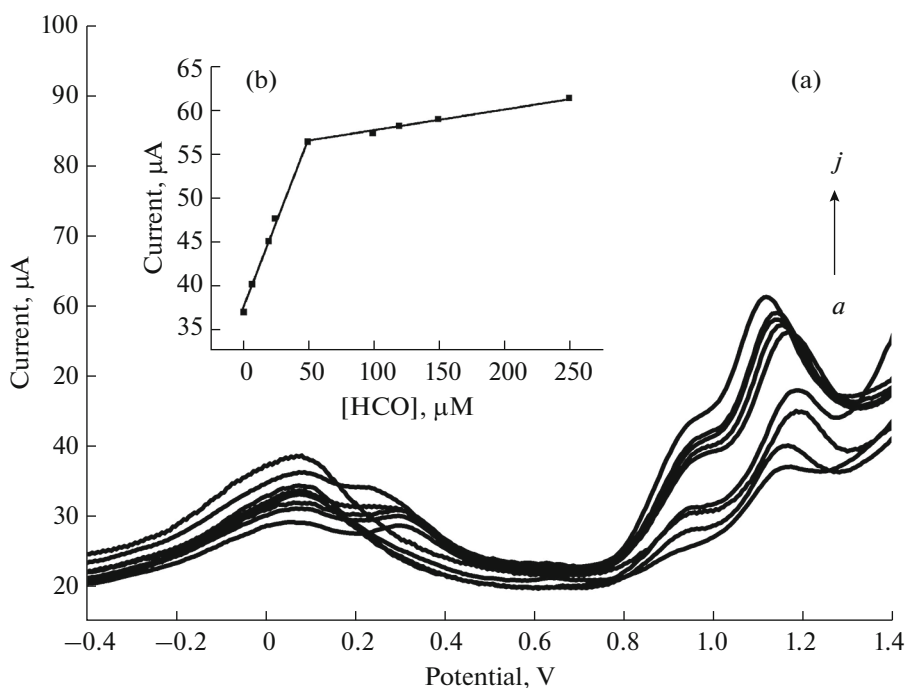
Fig. 11. (a) SWV curves of RGO–TiO$_2$ modified electrode in 0.1 M PBS solution of pH 6.00 containing 100 µM AA and various concentrations of HCQ containing $a \rightarrow j$ corresponding to: 1, 7.5, 20, 25, 50, 100, 120,150, and 250 µM. Inset: (b) showed the I_{pa} (µA) as a function of HCQ concentration (µM).

and HCQ respectively. Therefore, HCQ can be determined in the presence of AA on the surface of the modified electrode.

As shown in Figs. 11a, 11b, in the presence of a constant concentration of 100 µM of AA, the electrochemical response of HCQ increased linearly with the increase of the HCQ concentration, while the response of AA remained almost unchanged. The voltammogram clearly showed that the plot of peak current of HCQ (in the presence of AA) vs. HCQ concentration was composed of two linear segments with different slopes (the slope of the first linear segment and the second linear segment is 0.3955 and 0.0254 µA µM^{-1}), corresponding to two different ranges of substrate concentration, respectively, the first linear segment is 1–50 µM and the second linear segment is 50–250 µM. The decrease of sensitivity (slope) in the second linear range is most likely due to kinetic limitation. From the analysis of this data, we estimate that the calculated LOD of HCQ in the presence of AA is 0.0988 µM. The results suggested that even the presence of high concentration of AA did not strongly interfere with the determination of a low concentration of HCQ.

Stability and Repeatability of RGO–TiO$_2$/GCE

The stability of the sensor was further studied by maintaining the prepared modified electrode at room temperature for two weeks. The peak current is only reduced 5%. The intra-day and inter-day repeatability studies of the prepared electrode were carried out by consecutive measurements of 50 µM HCQ solutions in 0.1 M PBS of pH 6.00 under optimized conditions. The intra-day repeatability measurement was performed by 50 consecutive measurements of HCQ solutions and the relative standard deviation (RSD) was 3.5% ($n = 5$). The inter-day repeatability was evaluated in three consecutive days using the same parameters and the relative standard deviation (RSD) of 2.79% was obtained ($n = 5$). Obviously, the as-prepared RGO–TiO$_2$/GCE achieved sufficient stability and repeatability for detection of HCQ.

Interference Studies

The influence of the proposed sensor to some expected ionic species (K$^+$, Na$^+$, Cl$^-$, SO$_4^{2-}$, I$^-$) and selected organic compounds (UA, L-phenylalanine, ethanol, glucose) likely to be found in natural water samples for which the sensor developed herein is dedicated was evaluated. Under optimized conditions, the investigation was done by adding various interferences to a 0.1 M PBS of pH 6.00 solution in the presence of 50 µM HCQ. The RSD values obtained for each case are presented in Table 2. These results indicated that the RGO–TiO$_2$ modified electrode is selective for HCQ and its selectivity is not susceptible to interference.

Table 2. The selectivity of RGO–TiO$_2$/GCE for HCQ

Interfering substance	Added amount over HCQ concentration, mM	RSD, %
Na$^+$	5	0.37
Cl$^-$	5	0.37
K$^+$	5	2.59
I$^-$	5	2.59
SO$_4^{2-}$	5	3.33
Glucose	0.5	2.04
L-phenylalanine	0.5	2.59
Ethanol	0.5	2.96
UA	0.5	4.29

Analytical Application of the Proposed Modified Electrode in Medical Samples

To evaluate the validity of modified electrode in real examples, proper aliquots were extracted from the working solutions and voltammetrically determined by SWV technique in standard addition mode, and diluted with PBS to obtain the final concentrations within the calibration curve. As shown in Table 3, acceptable recoveries (98.5–99.4%) were obtained. The results indicated that the proposed modified elec-

trode could be applied for the routine analytical control of pharmaceuticals.

Analytical Application of the Proposed Modified Electrode in Urine Samples

To corroborate that the proposed method was sufficiently satisfactory and selective, the same urine samples were analyzed to determine HCQ. Different amounts of HCQ were spiked into the sample and analyzed by the designed electrochemical method. The results for determination of HCQ on the surface of RGO–TiO$_2$/GCE in real samples are given in Table 4. Satisfactory recovery results confirmed that the modified electrode retained its efficiency for determination of HCQ in urine samples.

CONCLUSIONS

In this paper, a novel self-assembly electrochemical sensor was successfully developed based on the RGO–TiO$_2$ NPs modified glassy carbon electrode for the determination of HCQ. After immobilized RGO–TiO$_2$ on the surface of GCE, the oxidation peak current of HCQ was significantly enhanced compared with the same bare electrode. The RGO–TiO$_2$ modified electrode had also been successfully used for sensitive and selective detection of HCQ in the presence of high concentration of AA. The coexisting AA does not interfere with the detection of HCQ. The proposed electrochemical sensor can selectively detect HCQ from 2.5×10^{-7} to 5.0×10^{-4} mol L^{-1} with a

Table 3. Results of the recovery analysis of HCQ spiked in tablet samples

Sample	Labeled/added, µmol L^{-1}	Found, µmol L^{-1}	Average recovery, %	RSD, %
1	20	18.2	98.5	1.50
2	50	48.6	99.1	0.93
3	80	77.4	98.6	1.44
4	100	98.8	99.4	0.60

Table 4. Results of the recovery analysis of HCQ spiked in urine samples

Sample	Labeled/added, µmol L^{-1}	Found, µmol L^{-1}	Average recovery, %	RSD, %
1	0	Not detected	–	–
2	25	25.89	103.6	3.70
3	50	48.04	96.1	3.30
4	75	71.13	94.8	1.71
5	100	96.13	96.1	2.56

detection limit of 12.5 nmol L^{-1}. The proposed method was successfully applied to the determination of HCQ in real samples and urine samples. It is worth noting that the novel electrochemical sensor proposed in this paper has the advantages of convenience, accuracy and high sensitivity, and is expected to be used for HCQ detection.

FUNDING

CONFLICT OF INTEREST

The authors declare no conflict of interest.

AUTHOR CONTRIBUTIONS

Huilan Zhang and Lu Cheng contributed equally.

REFERENCES

1. Mashhadizadeh, M.H. and Akbarian, M., Voltammetric determination of some anti-malarial drugs using a carbon paste electrode modified with $Cu(OH)_2$ nanowire, *Talanta,* 2009, vol. 78, p. 1440.

2. Pal, A., Pawar, A., Goswami, K., Sharmae, P., and Prasad, R., Hydroxychloroquine and Covid-19: a cellular and molecular biology based update, *Indian J. Clin. Biochem.,* 2020, vol. 35, no. 3, pp. 274–284.

3. Assalie, N.A., Durcan, R., and Durcan, L., Hydroxychloroquine-induced erythema multiforme, *J. Clin. Rheumatol.,* 2017, vol. 23, p. 127.

4. Merino, A.C., Molina, C.Z., and Suárez, P.D., Hydroxychloroquine, a potentially lethal drug, *Med. Intensiva,* 2017, vol. 41, p. 257.

5. Devnani, H., Satsangee, S.P., and Jain, R., A novel graphene-chitosan-Bi_2O_3 nanocomposite modified sensor for sensitive and selective electrochemical determination of a monoamine neurotransmitter epinephrine, *Ionics,* 2016, vol. 22, p. 943.

6. Khalil, M.M., Issa, Y., and El Sayed, G.A., Modified carbon paste and polymeric membrane electrodes for determination of hydroxychloroquine sulfate in pharmaceutical preparations and human urine, *RSC Adv.,* 2015, vol. 5, p. 83657.

7. Qu, Y., Noe, G., and Breaud, A.R., Development and validation of a clinical HPLC method for the quantification of hydroxychloroquine and its metabolites in whole blood, *Future Sci. OA*, vol. 1, p. fso.15.24.

8. Singh, A., Singh, C.L., and Gupta, R., Development and validation of reversed-phase high performance liquid chromatographic method for hydroxychloroquine sulphate, *Indian J. Pharm. Sci.,* 2015, vol. 77, p. 586.

9. Oliveira, A.R.M.D., Cardoso, C.D., and Bonato, P.S., Stereoselective determination of hydroxychloroquine and its metabolites in human urine by liquid-phase microextraction and CE, *Electrophoresis,* 2007, vol. 28, p. 1081.

10. Wang, L.Z., Ong, Y.L., and Chin, T.M., Method development and validation for rapid quantification of hydroxychloroquine in human blood using liquid chromatography-tandem mass spectrometry, *J. Pharm. Biomed.,* 2012, vol. 61, p. 8.

11. Füzéry, A.K., Breaud, A.R., and Emezienna, N., A rapid and reliable method for the quantitation of hydroxychloroquine in serum using turbulent flow liquid chromatography-tandem mass spectrometry, *Clin. Chim. Acta,* 2013, vol. 42, p. 79.

12. Deroco, P.B., Vicentini, F.C., and Oliveira, G.G., Square-wave voltammetric determination of hydroxychloroquine in pharmaceutical and synthetic urine samples using a cathodically pretreated boron-doped diamond electrode, *Electroanal. Chem.,* 2014, vol. 719, p. 19.

13. Ghoreishi, S.M., Attaran, A.M., and Amin, A.M., Multiwall carbon nanotube-modified electrode as a nanosensor for electrochemical studies and stripping voltammetric determination of an antimalarial drug, *RSC Adv.*, 2015, vol. 5, p. 14407.

14. Khoobi, A., Ghoreishi, S.M., and Behpour, M., Design and evaluation of a highly sensitive nanostructure-based surface modification of glassy carbon electrode for electrochemical studies of hydroxychloroquine in the presence of acetaminophen, *Colloids Surf. B,* 2014, vol. 123, p. 648.

15. Khoobi, A., Ghoreishi, S.M., and Behpour, M., Sensitive and selective determination of hydroxychloroquine in the presence of uric acid using anew nanostructure self-assembled monolayer modified electrode: optimization by multivariate data analysis, *Analyst,* 2014, vol. 139, p. 4064.

16. Wanag, A., Rokicka, P., and Wrobel, R.J., Antibacterial properties of TiO_2 modified with reduced grapheneoxide, *Ecotoxicol. Environ. Saf.,* 2018, vol. 147, p. 788.

17. Wang, M., Zhai, S., and Ye, Z., An electrochemical aptasensor based on a TiO_2/three-dimensional reduced graphene oxide/PP_y nanocomposite for the sensitive detection of lysozyme, *Dalton. T,* 2015, vol. 44, p. 6473.

18. Li, Y., Gu, Y., and Zheng, B., A novel electrochemical biomimetic sensor based on poly (Cu-AMT) with reduced graphene oxide for ultrasensitive detection of dopamine, *Talanta,* 2017, vol. 162, p. 80.

19. Manna, B. and Raj, C.R., Nanostructured sulfur-doped porous reduced graphene oxide for the ultrasensitive electrochemical detection and efficient removal of Hg(II), *ACS. Sustainability Chem. Eng.,* 2018, vol. 6, p. 6175.

20. Kim, T.W. and Park, S.J., Synthesis of reduced graphene oxide/thorn-like titanium dioxide nanofiber aerogels with enhanced electrochemical performance for supercapacitor, *J. Colloid. Interface Sci.,* 2017, vol. 486, p. 287.

21. Gülercan, D., Gergin, İ., and Sarac, A.S., Preparation and electrochemical performances of graphene oxide/PEDOT and reduced graphene oxide/PEDOT

nanofibers and nanocomposites, *Fiber. Polym.,* 2018, vol. 19, p. 2178.

22. Shang, H.Y., Ma, M., and Zhang, A.P., Self-assembled reduced graphene oxide-TiO₂ thin film for the enhanced photocatalytic reduction of Cr(VI) under simulated solar irradiation, *J. Nanosci. Nanotechnol.,* 2019, vol. 19, p. 3376.

23. Kang, X., Wang, J., and Wu, H., A graphene-based electrochemical sensor for sensitive detection of paracetamol, *Talanta,* 2010, vol. 81, p. 754.

24. Juana, R., Gregorio, C., and Lizcano, I., Electrochemical sensor for leukemia drug imatinib determination in urine by adsorptive striping square wave voltammetry using modified screen-printed electrodes, *Electrochim. Acta,* 2018, vol. 269, p. 668.

25. Shereen, M.A. and Amany, M.F., Electrochemical design of a new nanosensor based on cobalt nanoparticles, chitosan and MWCNT for the determination of daclatasvir: a hepatitis C antiviral drug, *RSC Adv.,* 2017, vol. 7, p. 1118.

26. Ferrari, A.G.M., Foster, C.W., Kelly, P.J., Brownson, D.A.C., and Banks, C.E., Determination of the electrochemical area of screen-printed electrochemical sensing platforms, *Biosensors,* 2018, vol. 8, p. 53.

27. Deroco, P.B., Oliveira, G.G., and Rocha-Filho, R.C., Square-wave voltammetric determination of hydroxychloroquine in pharmaceutical and synthetic urine samples using a cathodically pretreated boron-doped diamond electrode, *Electroanal. Chem.*, 2014, vol. 719, p. 19.